JACS
JOURNAL OF THE AMERICAN CHEMICAL SOCIETY

ARTICLE

pubs.acs.org/JACS

Size Fractionation of Graphene Oxide Sheets by pH-Assisted Selective Sedimentation

Xiluan Wang, Hua Bai, and Gaoquan Shi*

Key Laboratory of Bioorganic Phosphorus Chemistry & Chemical Biology, Department of Chemistry, Tsinghua University, Beijing 100084, People's Republic of China

Supporting Information

ABSTRACT: Graphene oxide (GO) sheets prepared by Hummers' method have been separated into two portions with large (f1) or small (f2) lateral dimensions from their aqueous dispersion. This method is based on the selective precipitation of GO sheets with lateral dimensions mostly (>90%) larger than 40 μm^2 at a pH value of 4.0 because of their larger hydrophobic planes and fewer hydrophilic oxygenated groups. The hydrazine reduced Langmuir–Blodgett (LB) films of f1 showed much higher conductivities than those of f2. Furthermore, the thin film of f1 prepared by filtration exhibited a smaller *d*-space and much higher tensile strength and modulus than those of f2 films. The one-step size fractionation method reported here is simple, cheap, efficient, and environmentally friendly, which can be used for the size fractionation of GO sheets in large scale.

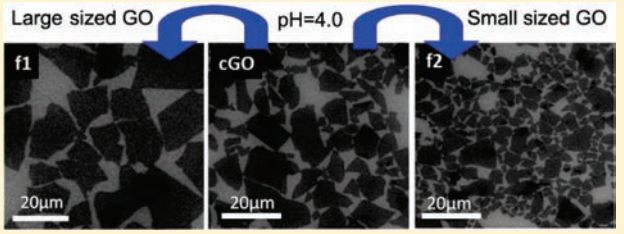

INTRODUCTION

Graphene, a one-atom thick sheet of sp^2-bonded carbon atoms, has potential applications in a variety of fields such as electronics, composites, sensors, and energy related systems because of its excellent electrical, optical, mechanical, and thermal properties.[1−12] It is known that the lateral dimensions of graphene sheets play an important role in controlling their properties and applications. For example, large-area graphene sheets are highly desirable for forming three-dimensional graphene-based networks[13] and fabricating optoelectronic devices,[14−18] while for the applications of biosensing and drug delivery, molecular sized graphene sheets are required for forming biocompatible fully functionalized surfaces.[9,19,20] It was also reported that the thermal conductivity of graphene is a strong function of its sheet size.[21,22] Accordingly, it is of significant importance to prepare graphene sheets with controlled sizes for their special applications. Hitherto, the most widely used method to mass production of graphene is the reduction of graphene oxide (GO).[1,5,7,14,15,23−44] Therefore, the sizes of the final chemical converted graphene (CCG) or reduced GO (rGO) sheets are mainly decided by those of their GO precursors. GO is usually synthesized by oxidation and exfoliation of natural graphite powder with various oxidants in acidic media. The typical method of synthesizing GO was developed by Hummers and co-workers.[45] Unfortunately, upon oxidation and sonication, the GO sheets are inevitably cut into small pieces with a wide size distribution. Although the size distribution of GO sheets can be narrowed to some extent by modifying the preparation conditions such as using different oxidants or changing the reaction time or media,[16,44,46,47] the results are still unsatisfactory. Particularly, all of the GO products prepared by these techniques contained small GO sheets with lateral dimensions in submicrometer scale. Thus, a convenient and high-output method for controlling GO sizes and their distributions remains to be exploited.

Recently, a density gradient ultracentrifugation (DGU) technique has been applied to separate GO sheets with different sizes.[9] Sun et al. also developed a density gradient ultracentrifugal rate (DGUR) method for the fractionation of CCG sheets.[48] However, the severely high centrifugation rate, the small size of centrifuge tube, and the use of specialized gradient medium limited large-scale production of GO sheets with desired sizes. Here, we report a rapid and simple size separation method based on the pH-dependent amphiphilicity of GO sheets. We found that the pH-induced sedimentation of GO sheets depended on their sizes. Thus, by adjusting the pH value of a GO dispersion, size fractionation of GO sheets can be easily realized. This technique can be used to produce GO sheets with large lateral sizes (mostly larger than 40 μm^2) and narrow size distribution in large quantity. The thin Langmuir–Blodgett (LB) and paper-like films based on the large and narrow-distributed GO or rGO sheets showed greatly improved mechanical or electrical properties.

EXPERIMENTAL SECTION

Preparation of GO. GO was prepared by Hummers' method, and the procedures are briefly described as follows.[45] Graphite powder (25 meshes, 33.0 g) and sodium nitrate (1.5 g) were mixed in sulfuric acid (70 mL, 98 wt %) under stirring and cooled by using an ice bath.

Received: January 9, 2011
Published: March 30, 2011

dx.doi.org/10.1021/ja200218y | J. Am. Chem. Soc. 2011, 133, 6338–6342

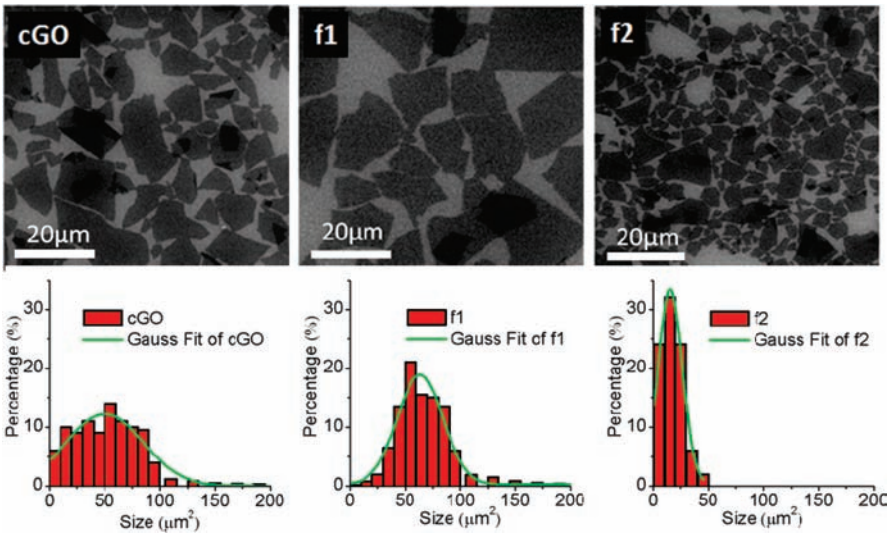

Figure 1. SEM image and corresponding histogram of GO size distribution (under the SEM image) of cGO, f1, or f2 LB monolayer on a silicon substrate. The histograms of GO size distributions were obtained by counting more than 1000 sheets for each sample. The Gaussian fit curve of each sample is colored in green.

Under vigorous agitation, potassium permanganate (9.0 g) was added slowly to prevent the temperature from exceeding 20 °C. Successively, the reaction system was transferred to a 35 ± 5 °C water bath for 0.5 h, forming a thick paste. Next, 150 mL of water was gradually added, and the solution was stirred for 15 min at 90 ± 5 °C. Additional 500 mL of water was added and treated with 15 mL of H_2O_2 (3 wt %), turning the color of the solution from dark brown to yellow. The mixture was filtered and washed with 1:10 HCl aqueous solution (250 mL) to remove the acid. The resulting solid was dried in air and diluted. A GO suspension in water (1 mg/mL) was obtained after ultrasonication for 30 min, followed by centrifugation (4000 rpm, 30 min) to remove the residual graphite and graphite oxide. Finally, it was purified by dialysis for 1 week to remove the remaining metal species.

Size Fractionation of GO. The pH value of an aqueous dispersion of the GO prepared by Hummers' method described above (1 mg/mL or lower) was adjusted to 4.0 using 1 M HCl and aged for over 4 h. During this process, part of the GO was precipitated. Both the sediment and the residual dispersion were collected and dialyzed with deionized water to remove the inorganic additives. These two GO fractions are defined as f1 and f2, respectively.

Preparation of the Langmuir–Blodgett (LB) Films of GO or rGO. One volume aqueous dispersion of GO (1 mg/mL) was diluted with 5 volumes methanol without sonication for keeping the sizes of the GO sheets.[30] For LB, the trough (KSV Minitrough, 10 cm × 25 cm) was carefully cleaned and then filled with deionized water. GO solution was dropped into the trough with a speed of 100 μL/min and spread onto the water surface using a glass syringe to a total volume of 8–10 mL. The surface pressure was monitored using a tensiometer attached to a Wilhelmy plate. The film was compressed by barriers at a speed of 20 cm^2/min. The GO monolayer was transferred, typically midway, by vertically dipping the substrate into the trough and slowly pulling it up (2 mm/min). Quartz or silicon sheets were used as the substrates, and they were treated with 1:1:5 NH_4OH:H_2O_2:H_2O (by volume) and washed repeatedly with deionized water before use. Two- and three-layer GO LB films were prepared by drying the as-formed films in an oven at 80 °C for 1 h and then depositing another layer of GO under the same condition. Thin GO films assembled on quartz substrates by LB technique were reduced by hydrazine vapor at 100 °C for 1 h to form rGO films.

Preparation of GO Papers. Free-standing GO papers were prepared by vacuum filtration of 15 mL of GO aqueous dispersions (1 mg/mL) through porous poly(tetraflouroethylene) (PTFE) membranes (47 mm in diameter and 0.2 μm in pore size). Successively, they were dried overnight under vacuum at 50 °C before characterization.

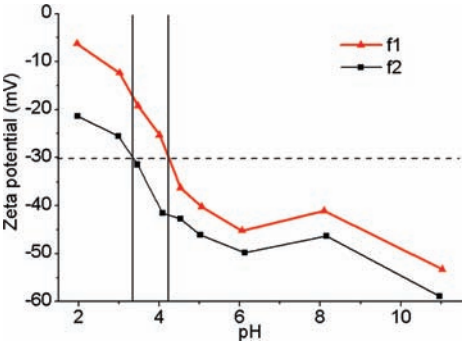

Figure 2. Zeta potential of f1 or f2 aqueous dispersion as a function of its pH value.

Characterization. The pH value of each sample was measured by a pH meter (PHS-3C). A scanning electron microscope (SEM, Hitachi S-5500) and an atomic force microscope (AFM, Nanoscope III Multi-Mode) in tapping mode were used to characterize GO sheet sizes and thickness. The zeta (ζ) potentials of GO aqueous dispersions with various pH values were measured by the use of a zetasizer nanosystem (Malvern Instruments). The pH values of the GO dispersions were modulated by adding 1 M HCl or KOH. The X-ray diffraction (XRD) patterns were recorded on a D8 Advance X-ray diffractometer (Bruker) with Cu Kα radiation (λ = 1.5418 Å). The X-ray photoelectron energy spectra (XPS) were performed using a ULVAC-PHI XPS spectrometer (Thermo Electron) with Al Kα radiation. The mechanical properties of GO papers were tested by the use of a model 3342 universal mechanical testing machine (Instron, U.S.) at a stretching rate of 0.5 mm/min. GO papers with thicknesses of 10–15 μm were cut into strips with 2–3 mm in width and 20–25 mm in length and used as the specimens. The reported data were the average of four tests of the same sample. All of the failures occurred at the middle regions of the specimens. The sheet resistances of rGO LB films were measured by using conventional four-probe technique, and their transmittances were evaluated by using a UV–vis spectrometer (Hitachi U-3900). All measurements were

dx.doi.org/10.1021/ja200218y |J. Am. Chem. Soc. 2011, 133, 6338–6342

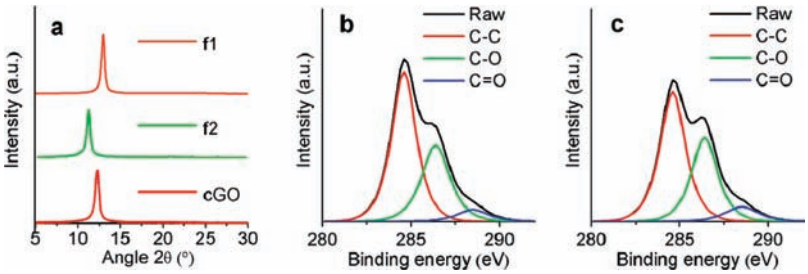

Figure 3. (a) XRD patterns of cGO, f1, and f2 papers prepared by vacuum filtration and (b,c) the C 1s XPS spectra of (b) f1 and (c) f2 papers.

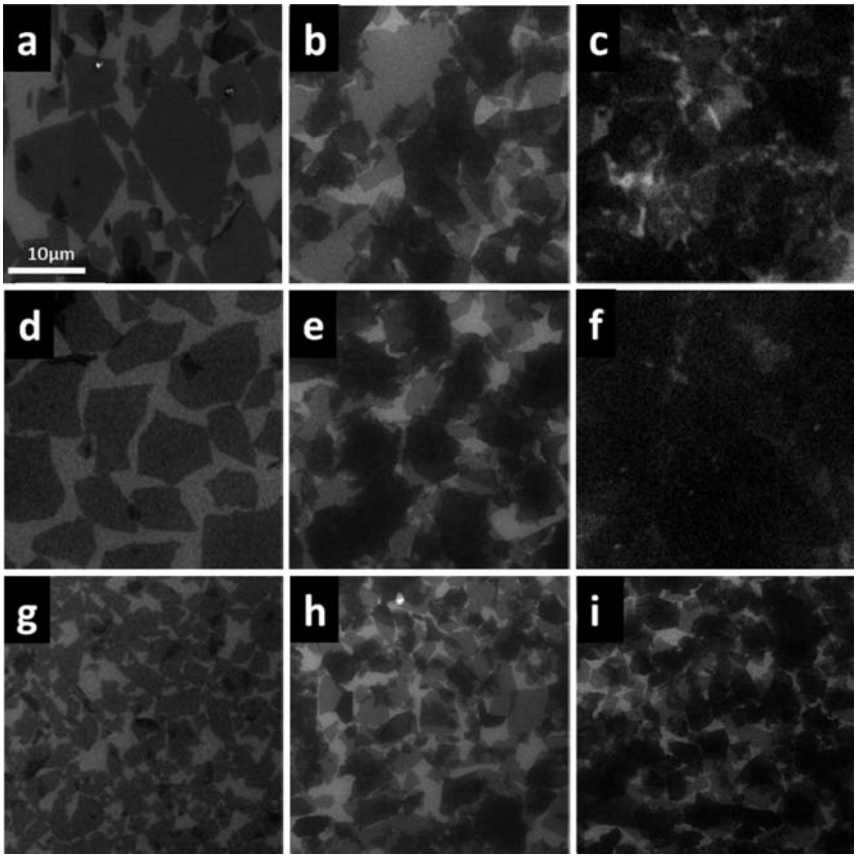

Figure 4. Typical SEM images of the LB films of rGO prepared from cGO (a−c), f1 (d−f), and f2 (g−i) with one- (a,d,g), two- (b,e,h), and three- (c,f,i) rGO layers on quartz substrates. The images have the same magnifications, scale bar = 10 μm.

conducted at room temperature and under an environment with humidity around 20%.

RESULTS AND DISCUSSION

A GO sheet can be recognized as a single layer graphite bring various hydrophilic oxygenated functional groups.[30,36,49−52] The hydroxyl and epoxide groups are mainly on the basal planes, and ionizable carboxylic acid groups are mostly at the edges of GO sheets.[53] Thus, GO sheets can be dispersed in water to form a stable colloidal dispersion. It was also believed that the electrostatic repulsion between GO sheets, resulting from their ionized carboxyl groups, prevented their aggregation in aqueous medium.[7] The edge-to-area ratio of a GO sheet increases with the decrease of its lateral dimension. Thus, in the aqueous media with the same pH value, the smaller GO sheets should have higher solubility than that of their larger counterparts because of higher densities of ionized −COOH groups. Furthermore, the solubility

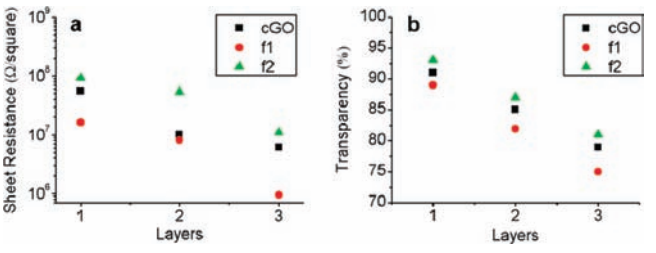

Figure 5. (a) Sheet resistances and (b) transmittances at 550 nm of reduced cGO, f1, and f2 films with different LB layers on quartz substrates.

dx.doi.org/10.1021/ja200218y |J. Am. Chem. Soc. 2011, 133, 6338–6342

of GO sheets in water also decreases with the decrease of the pH value of their dispersion. This is mainly due to that the repulsion force between GO sheets is weakened by the protonation of their carboxyl groups. Therefore, we can acidify a GO dispersion to proper pH values for selectively precipitating large GO sheets. This process is similar to that of fractionating a polymer with different molecular weights by mixing its solution with a poor solvent. For our GO dispersions prepared by Hummers' method, the pH range suitable for GO size fractionation was tested to be 3.34−4.24, and we call it the "pH window". Actually, a crude GO (cGO) colloidal dispersion was separated into two portions by adjusting its pH value to 4.0 with 1 M HCl and collecting the precipitant of larger sized GO sheets (f1) and the residual stable dispersion of smaller sized GO sheets (f2). The successful size fractionation can be reflected by the scanning electron microscope (SEM) images shown in Figure 1. The samples used for SEM studies were prepared by LB assembling the GO sheets of cGO, f1, or f2 on silicon substrates at the same regions of isotherm surface/area curves that GO sheets were close-packed (Figures S1, S2). According to the SEM images and their size distribution histograms, the sizes of cGO sheets are widely distributed from <1 to over 200 μm^2. However, the GO sheets are mostly (>90%) larger than 40 μm^2 in f1 and smaller than 50 μm^2 in f2. The Gauss fits of cGO, f1, and f2 indicate that their maximum distributions of GO sizes are 49, 65, and 15 μm^2, respectively, and their half band widths were measured to be 69.9, 41.4, and 22.2 μm^2, correspondingly. These results demonstrate that the GO sheets of cGO have been fractionated into two portions with large (f1, mostly >40 μm^2) or small (f2, <50 μm^2) lateral dimensions, and f1 and f2 have much narrower size distributions than that of cGO.

The mechanism of the pH-induced size fractionation of GO sheets was studied by ζ potential measurements. As shown in Figure 2, the ζ potentials of f1 and f2 dispersions decrease with the increase of their pH values because of the ionization of −COOH groups. It was reported that a GO dispersion was stable only as its ζ potential < −30 mV.[7] In the "pH window" of 3.34−4.24, the ζ potential of f1 is higher than −30 mV, and that of f2 is lower than this value (Figure 2). Therefore, within the "pH window", cGO can be fractionated by selectively precipitating its large GO sheets. Here, we should figure out that the GO dispersions with pH values beyond the "pH window" can also be size fractionated under more serious conditions, such as using DGU or DGUR techniques. However, here, we offer a simple one-step method by just adjusting the pH value of GO dispersion, which shows great potential of size fractionation of GO sheets in large scale.

The sizes of GO sheets have strong effects on the structures and properties of their self-assembled films. GO sheets can be assembled into paper-like films by filtration.[2] The structures of our GO papers were studied by X-ray diffraction (XRD). The XRD patterns of cGO, f1, and f2 papers (Figure 3a) show peaks at 2θ = 12.3°, 13.0°, and 12.0°, respectively, and their d-spaces are calculated to be 0.72, 0.68, and 0.74 nm, correspondingly. The half peak widths of the XRD peaks were measured to be 0.53°, 0.48°, and 0.68°, respectively. The f1 paper has the narrowest XRD peak and the shortest d-space. According to previous reports, the relative humidity[54] and the stacking situation[2] of GO sheets are main factors for controlling the d-space of a layered GO paper. Under the same humidity, the confined water in the interlamellar spaces of GO papers with different sized sheets predominantly depends on their abilities of trapping water molecules.[54] XPS results indicate that f1 brings fewer oxygenated groups than does f2 (Figure 3b,c). Thus, it can absorb less water through hydrogen bonding, which leads to a smaller d-space. On the other hand, the larger GO sheets in f1 also resulted in the formation of layered film with fewer structural defects, which further reduces the d-space and the width of the XRD peak.[53]

The large GO sheets and compact structure of f1 paper also greatly improved its mechanical property (Figure S3). The tensile strength (δ) or tensile modulus (E) of f1 paper (δ= 90.4 M Pa, E = 7.6 GPa) was measured to be about twice that of f2 paper (δ = 42.3 MPa, E = 3.4 GPa). Furthermore, the mechanical property of f1 paper is also much higher than that of cGO paper (δ = 65.6 MPa, E = 5.0 GPa). This is mainly due to that f1 paper has the most compact structure and the fewest defects because of its large GO sheets as described above.

The morphology, optical, and electrical properties of the LB films of rGO also depend strongly on the sizes of their GO precursors. The sheet resistances of hydrazine-reduced cGO, f1, and f2 monolayers were measured to be 54.9, 16.2, and 91.8 MΩ/sq, respectively. The lowest sheet resistance of reduced f1 monolayer is attributed to its largest rGO sheets with the fewest structural defects. Furthermore, the larger rGO sheets can also form monolayer with lower contact resistance because of its fewer sheet contacts (Figure 4). The conductivities of the rGO films increase with their LB layer number (Figure 5a). The sheet resistance of three-layered rGO film of f1 can achieve 0.95 MΩ/sq, which is significantly lower than that of 10.9 MΩ/sq for reduced f2 and 6.2 MΩ/sq for reduced cGO (Figure 5a). On the other hand, increasing the number of LB layers decreases the transmittance of reduced GO film (Figure 5b). For example, the transmittance of reduced f1 film at 550 nm was measured to be 89% for monolayer and 75% for a three-layered film. The LB film of reduced f1 with a given layer number has the most compact morphology (Figure 4) and the lowest transmittance (Figure 5).

CONCLUSION

We have successfully developed a universal technique for size fractionation of GO sheets by just adjusting the pH value of GO dispersion. This method is simple, cheap, and environmentally friendly, and it can be used to treat large amounts of GO in one step. The lateral dimensions of GO sheets have strong effects on the structures and properties of the self-assembled GO films. Larger GO sheets favor the formation of paper-like films with more tight and perfect structures, which greatly improved their mechanical properties. Furthermore, the LB films of larger GO sheets also showed higher conductivities after chemical reduction because of their more compact morphology, fewer structural defects, and lower contact resistances.

ASSOCIATED CONTENT

Supporting Information. Figure S1, isothermal surface pressure/area plots of forming close packed monolayers of cGO, f1, and f2; Figure S2, AFM image of GO sheets of typical f1; and Figure S3, the tensile stress−strain curves of cGO, f1, and f2 papers. This material is available free of charge via the Internet at http://pubs.acs.org.

AUTHOR INFORMATION

Corresponding Author
gshi@tsinghua.edu.cn

■ ACKNOWLEDGMENT

This work was supported by the Natural Science Foundation of China (91027028, 50873092). We are grateful to Prof. Xiufeng Han (Institute of Physics, Chinese Academy of Science) for providing his LB instrument for our study.

■ REFERENCES

(1) Stankovich, S.; Dikin, D. A.; Dommett, G. H. B.; Kohlhaas, K. M.; Zimney, E. J.; Stach, E. A.; Piner, R. D.; Nguyen, S. T.; Ruoff, R. S. *Nature* **2006**, *442*, 282.
(2) Dikin, D. A.; Stankovich, S.; Zimney, E. J.; Piner, R. D.; Dommett, G. H. B.; Evmenenko, G.; Nguyen, S. T.; Ruoff, R. S. *Nature* **2007**, *448*, 457.
(3) Geim, A. K.; Novoselov, K. S. *Nat. Mater.* **2007**, *6*, 183.
(4) Balandin, A. A.; Ghosh, S.; Bao, W.; Calizo, I.; Teweldebrhan, D.; Miao, F.; Lau, C. N. *Nano Lett.* **2008**, *8*, 902.
(5) Eda, G.; Fanchini, G.; Chhowalla, M. *Nat. Nanotechnol.* **2008**, *3*, 270.
(6) Lee, C.; Wei, X.; Kysar, J. W.; Hone, J. *Science* **2008**, *321*, 385.
(7) Li, D.; Muller, M. B.; Gilje, S.; Kaner, R. B.; Wallace, G. G. *Nat. Nanotechnol.* **2008**, *3*, 101.
(8) Li, X.; Wang, X.; Zhang, L.; Lee, S.; Dai, H. J. *Science* **2008**, *319*, 1229.
(9) Sun, X.; Liu, Z.; Welsher, K.; Robinson, J.; Goodwin, A.; Zaric, S.; Dai, H. J. *Nano Res.* **2008**, *1*, 203.
(10) Westervelt, R. M. *Science* **2008**, *320*, 324.
(11) Fowler, J. D.; Allen, M. J.; Tung, V. C.; Yang, Y.; Kaner, R. B.; Weiller, B. H. *ACS Nano* **2009**, *3*, 301.
(12) Wang, L.; Lee, K.; Sun, Y.-Y.; Lucking, M.; Chen, Z.; Zhao, J. J.; Zhang, S. B. *ACS Nano* **2009**, *3*, 2995.
(13) Xu, Y. X.; Sheng, K. X.; Li, C.; Shi, G. Q. *ACS Nano* **2010**, *4*, 4324.
(14) Becerril, H. A.; Mao, J.; Liu, Z.; Stoltenberg, R. M.; Bao, Z.; Chen, Y. *ACS Nano* **2008**, *2*, 463.
(15) Wang, X.; Zhi, L. J.; Mullen, K. *Nano Lett.* **2008**, *8*, 323.
(16) Zhao, J. P.; Pei, S. F.; Ren, W. C.; Gao, L. B.; Cheng, H. M. *ACS Nano* **2010**, *4*, 5245.
(17) Chang, H. X.; Wang, G. F.; Yang, A.; Tao, X. M.; Liu, X. Q.; Shen, Y. D.; Zheng, Z. J. *Adv. Funct. Mater.* **2010**, *20*, 2893.
(18) Su, C. Y.; Xu, Y. P.; Zhang, W. J.; Zhao, J. W.; Liu, A. P.; Tang, X. H.; Tsai, C. H.; Huang, Y. Z.; Li, L. J. *ACS Nano* **2010**, *4*, 5285.
(19) Liu, Z.; Robinson, J. T.; Sun, X. M.; Dai, H. J. *J. Am. Chem. Soc.* **2008**, *130*, 10876.
(20) Agarwal, S.; Zhou, X. Z.; Ye, F.; He, Q. Y.; Chen, G. C. K.; Soo, J.; Boey, F.; Zhang, H.; Chen, P. *Langmuir* **2010**, *26*, 2244.
(21) Nika, D. L.; Ghosh, S.; Pokatilov, E. P.; Balandin, A. A. *Appl. Phys. Lett.* **2009**, *94*, 203103.
(22) Ghosh, S.; Bao, W. Z.; Nika, D. L.; Subrina, S.; Pokatilov, E. P.; Lau, C. N.; Balandin, A. A. *Nat. Mater.* **2010**, *9*, 555.
(23) Schniepp, H. C.; Li, J. L.; McAllister, M. J.; Sai, H.; Herrera-Alonso, M.; Adamson, D. H.; Prud'homme, R. K.; Car, R.; Saville, D. A.; Aksay, I. A. *J. Phys. Chem. B* **2006**, *110*, 8535.
(24) Stankovich, S.; Dikin, D. A.; Piner, R. D.; Kohlhaas, K. A.; Kleinhammes, A.; Jia, Y.; Wu, Y.; Nguyen, S. T.; Ruoff, R. S. *Carbon* **2007**, *45*, 1558.
(25) Fan, X. B.; Peng, W. C.; Li, Y.; Li, X. Y.; Wang, S. L.; Zhang, G. L.; Zhang, F. B. *Adv. Mater.* **2008**, *20*, 4490.
(26) Si, Y.; Samulski, E. T. *Nano Lett.* **2008**, *8*, 1679.
(27) Wang, G. X.; Yang, J.; Park, J.; Gou, X. L.; Wang, B.; Liu, H.; Yao, J. *J. Phys. Chem. C* **2008**, *112*, 8192.
(28) Williams, G.; Seger, B.; Kamat, P. V. *ACS Nano* **2008**, *2*, 1487.
(29) Chen, Y.; Zhang, X.; Yu, P.; Ma, Y. W. *Chem. Commun.* **2009**, 4527.
(30) Cote, L. J.; Kim, F.; Huang, J. X. *J. Am. Chem. Soc.* **2009**, *131*, 1043.
(31) Gao, W.; Alemany, L. B.; Ci, L. J.; Ajayan, P. M. *Nat. Chem.* **2009**, *1*, 403.
(32) Kim, M. C.; Hwang, G. S.; Ruoff, R. S. *J. Chem. Phys.* **2009**, *131*, 064704.
(33) Lee, V.; Whittaker, L.; Jaye, C.; Baroudi, K. M.; Fischer, D. A.; Banerjee, S. *Chem. Mater.* **2009**, *21*, 3905.
(34) Li, X. L.; Wang, H. L.; Robinson, J. T.; Sanchez, H.; Diankov, G.; Dai, H. J. *J. Am. Chem. Soc.* **2009**, *131*, 15939.
(35) Mattevi, C.; Eda, G.; Agnoli, S.; Miller, S.; Mkhoyan, K. A.; Celik, O.; Mostrogiovanni, D.; Granozzi, G.; Garfunkel, E.; Chhowalla, M. *Adv. Funct. Mater.* **2009**, *19*, 2577.
(36) Park, S.; Ruoff, R. S. *Nat. Nanotechnol.* **2009**, *4*, 217.
(37) Ramesha, G. K.; Sampath, S. *J. Phys. Chem. C* **2009**, *113*, 7985.
(38) Shin, H. J.; Kim, K. K.; Benayad, A.; Yoon, S. M.; Park, H. K.; Jung, I. S.; Jin, M. H.; Jeong, H. K.; Kim, J. M.; Choi, J. Y.; Lee, Y. H. *Adv. Funct. Mater.* **2009**, *19*, 1987.
(39) Tung, V. C.; Allen, M. J.; Yang, Y.; Kaner, R. B. *Nat. Nanotechnol.* **2009**, *4*, 25.
(40) Wang, Z. J.; Zhou, X. Z.; Zhang, J.; Boey, F.; Zhang, H. *J. Phys. Chem. C* **2009**, *113*, 14071.
(41) Gao, X. F.; Jang, J.; Nagase, S. *J. Phys. Chem. C* **2010**, *114*, 832.
(42) Loh, K. P.; Bao, Q. L.; Ang, P. K.; Yang, J. X. *J. Mater. Chem.* **2010**, *20*, 2277.
(43) Mohanty, N.; Nagaraja, A.; Armesto, J.; Berry, V. *Small* **2010**, *6*, 226.
(44) Zhou, X. F.; Liu, Z. P. *Chem. Commun.* **2010**, *46*, 2611.
(45) Hummers, W. S.; Offeman, R. E. *J. Am. Chem. Soc.* **1958**, *80*, 1339.
(46) Su, C. Y.; Xu, Y. P.; Zhang, W. J.; Zhao, J. W.; Tang, X. H.; Tsai, C. H.; Li, L. J. *Chem. Mater.* **2009**, *21*, 5674.
(47) Zhang, L.; Liang, J. J.; Huang, Y.; Ma, Y. F.; Wang, Y.; Chen, Y. S. *Carbon* **2009**, *47*, 3365.
(48) Sun, X. M.; Luo, D. C.; Liu, J. F.; Evans, D. G. *ACS Nano* **2010**, *4*, 3381.
(49) Li, X. L.; Zhang, G. Y.; Bai, X. D.; Sun, X. M.; Wang, X. R.; Wang, E.; Dai, H. J. *Nat. Nanotechnol.* **2008**, *3*, 538.
(50) Li, D.; Kaner, R. B. *Science* **2008**, *320*, 1170.
(51) Kim, J.; Cote, L. J.; Kim, F.; Yuan, W.; Shull, K. R.; Huang, J. X. *J. Am. Chem. Soc.* **2010**, *132*, 8180.
(52) Kim, F.; Cote, L. J.; Huang, J. *Adv. Mater.* **2010**, *22*, 1954.
(53) Szabo, T.; Berkesi, O.; Forgo, P.; Josepovits, K.; Sanakis, Y.; Petridis, D.; Dekany, I. *Chem. Mater.* **2006**, *18*, 2740.
(54) Lerf, A.; Buchsteiner, A.; Pieper, J.; Schottl, S.; Dekany, I.; Szabo, T.; Boehm, H. P. *J. Phys. Chem. Solids* **2006**, *67*, 1106.